Covert Communication of STAR-RIS Aided NOMA Networks

Xingwang Li, *Senior Member, IEEE,* Zhifa Tian, Wenjing He, Gaojie Chen, *Senior Member, IEEE,* M. Cenk Gursoy, *Senior Member, IEEE,* Shahid Mumtaz, *Senior Member, IEEE,* and Arumugam Nallanathan, *Fellow, IEEE*

***Abstract*—This paper investigates covert communication in simultaneously transmitting and reflecting reconfigurable intelligent surface (STAR-RIS) assisted non-orthogonal multiple access (NOMA) systems, assuming for the sake of being more practical that the successive interference cancellation (SIC) is defective. To assess the covertness performance of the considered system, we first derive closed-form expressions for the detection error probability, the optimal judgment threshold and the average minimum detection error probability of the warden, as well as the outage probability of the NOMA user pair. Then an optimization problem to maximize the effective covert rate (ECR) is proposed. Simulation results verify that the maximum ECR of the considered system could be increased by varying the different proportions of transmission and reflection components of the STAR-RIS.**

***Index Terms*—Covert communication, detection error probability, effective covert rate, NOMA, STAR-RIS.**

I. Introduction

Reconfigurable intelligent surfaces (RIS) is one of the outstanding technologies to enhance wireless network performance. The RIS contains a large number of passive reflective components that can dynamically modify the radio channels by altering the phase shift and amplitude [1]. However, most of the existing research works consider that the transmitter and receiver must be located on the same side of the RIS, but this geographical limitation may not always be met in practice and severely limits the flexibility and effectiveness of RIS deployment. To break the bottleneck of the coverage, the authors of [2] proposed a novel idea of concurrently transmitting and reflecting RIS (STAR-RIS). The STAR-RIS provided full spatial coverage by reflecting and refracting the incident signal to the users on the same and opposite sides of the source [3].

Meanwhile, non-orthogonal multiple access (NOMA) is widely regarded as a promising multiple access candidate for the sixth generation networks due to its high spectral efficiency [4]. The introduction of STAR-RIS in NOMA networks will have the advantages of enhancing the coverage area, improving the quality of service and reducing power consumption [5]. Indeed, several studies have recently been conducted to demonstrate the superiority of the combination of STAR-RIS and NOMA [6]. The authors of [7] analyzed the outage probability (OP) and ergodic rate of a pair of users in a STAR-RIS NOMA network and showed that the network can enhance the reliability of the communication link. Furthermore, Liu *et al.* [8] used the effective capacity (EC) as a metric and analytically concluded that the EC of the considered system was superior to that of the STAR-RIS orthogonal multiple access network and the conventional RIS network. Wang *et al.* [9] proposed a mode switching STAR-RIS NOMA network over spatially correlated channels and show that channel correlation degrades performance in terms of OP. Considering residual hardware impairments (RHIs) at all nodes, the authors in [10] explored the secure performance of downlink STAR-RIS NOMA networks by deriving secrecy outage probability (SOP).

In recent years, covert communication has emerged as a new security paradigm to ensure that the information transmission between two users has a negligible probability of being detected at the warden. The studies on covert communication in NOMA-based networks have shown that one can not only satisfy the covert nature of the communication but also increase the rate of information transmission [11]. In [12], Zhang *et al.* investigated covert communication in the NOMA system with user's channel knowledge uncertainty and considered the situation where the optimal antenna is not accessible for selection in a multi-antenna transmitter. On the other hand, without having to change the associated protocols and hardware, the addition of RIS to an existing system can enhance covert communication performance. For example, the authors of [13] revealed that the integration an RIS into communication networks can enhance covertness performance. Moreover, due to the inherent uncertainty in non-orthogonal transmission and RIS phase shift uncertainty, implementing covert communication in a combined RIS and NOMA scheme is more practical and simpler to accomplish [14].

Although there are many benefits to combining STAR-RIS with NOMA, the investigation of covert communication in STAR-RIS NOMA networks is still in its infancy. Compared to the existing works in [8] and [10], this paper has three main differences. Firstly, we consider the covert communication

Xingwang Li, Zhifa Tian and Wenjing He are with the School of Physics and Electronic Information Engineering, Henan Polytechnic University, Jiaozuo, China (email:lixingwangbupt@gmail.com, tianzhifa@home.hpu.edu.cn, hewenjing07@163.com).

Gaojie Chen is with the 5GIC & 6GIC, Institute for Communication Systems (ICS), University of Surrey, Guildford, GU2 7XH, United Kingdom (email: gaojie.chen@surrey.ac.uk).

M. Cenk Gursoy is with the Department of Electrical Engineering and Computer Science, Syracuse University, Syracuse, NY, 13244 USA (mcgursoy@syr.edu).

Shahid Mumtaz is with the Instituto de Telecomunicacoes, 3810078 Aveiro, Portugal (e-mail: smumtaz@av.it.pt).

Arumugam Nallanathan is with the School of Electronic Engineering and Computer Science, Queen Mary University of London, London E1 4NS, UK (a.nallanathan@qmul.ac.uk).

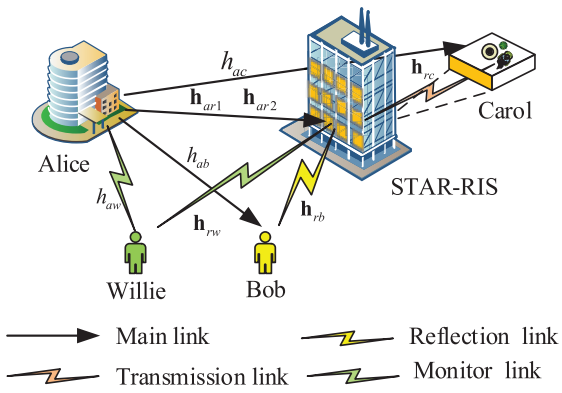

Fig. 1. System model of STAR-RIS NOMA network.

problem in STAR-RIS assisted NOMA networks, which has not been studied in previous literature. Secondly, this paper proposes a covert communication strategy that uses non-orthogonal transmission and STAR-RIS techniques without external interference sources. Moreover, we also consider non-ideal factors that exist in practical communication, such as imperfect successive interference cancellation (SIC). Therefore, this paper carries out the covertness analysis in STAR-RIS assisted NOMA networks. The main contributions are as follows: 1) the detection error probability (DEP) of the warden is determined analytically; 2) an optimization problem to maximize the effective covert rate (ECR) is proposed; 3) the impact of the number of STAR-RIS elements on the covertness performance is analyzed. Finally, our analysis is verified by numerical simulations.

II. System Model

A. Network Model

We consider covert communication of relatively stationary nodes in downlink STAR-RIS assisted NOMA networks, which consists of a source (Alice), a STAR-RIS with K elements, a warden (Willie), a covert user (Bob) as the near user and a public indoor user (Carol) as the far user [15].[1] A more general communication scenario are designed in which Bob and Carol can receive signals from both Alice and STAR-RIS. Specifically, Bob and Carol are located at opposite ends of the STAR-RIS and they can independently receive the signal due to the reflective and refractive transmission of the STAR-RIS. In addition, Willie is located on the front of the STAR-RIS and can receive signals from both Alice and the STAR-RIS.

In this study, we have the following assumptions: 1) We use the STAR-RIS mode switching protocol since it is convenient to deploy, thus splitting the K elements into two subsets, i.e., K_n elements serving Bob and K_m elements serving Carol; 2) Each channel follows as Rayleigh fading channel.[2] The channel coefficients of the Alice-STAR-RIS link, STAR-RIS-Bob link, STAR-RIS-Willie link, STAR-RIS-Carol link and Alice-Bob link, Alice-Willie link are expressed as $\mathbf{h}_i \sim \mathcal{CN}(0, \lambda_i \mathbf{I}_j)$, $i \in \{ar, rb, rw, rc\}$, $j \in \{K_n, K_m\}$, $h_f \sim \mathcal{CN}(0, \lambda_f)$, $f \in \{ab, aw, ac\}$; 3) The distances of the above links are respectively denoted as d_i and d_f; 4) All nodes are single antenna devices except STAR-RIS; 5) Alice only knows the statistical channel state information (CSI) of the Alice-Willie link.

[1]This work can be extended to multiple users, but to give a clear analysis and design, we just use two users here.

[2]To obtain a tractable solution and show insights, we choose Rayleigh fading in this work. In the future, we will further investigate generalized channel models such as Rician and Nakagami-m fading model.

B. Transmission Phase

Alice sends a common signal $s_c(n)$ and a covert signal $s_b(n)$ to Carol and Bob with $\mathbb{E}\left(|s_c|^2\right) = \mathbb{E}\left(|s_b|^2\right) = 1$, respectively. Consequently, the signals received at Bob and Carol are respectively given by

$$y_b(n) = \left(\frac{h_{ab}}{d_{ab}^{\frac{\alpha_{ab}}{2}}} + \frac{\mathbf{h}_{ar_1}^H \Theta_R \mathbf{h}_{rb}}{d_{ar}^{\frac{\alpha_{ar}}{2}} d_{rb}^{\frac{\alpha_{rb}}{2}}}\right) \times \left(\sqrt{P_c} s_c(n) + \sqrt{P_b} s_b(n)\right) + z_b(n), \tag{1}$$

and

$$y_c(n) = \left(\frac{h_{ac}}{d_{ac}^{\frac{\alpha_{ac}}{2}}} + \frac{\mathbf{h}_{ar_2}^H \Theta_T \mathbf{h}_{rc}}{d_{ar}^{\frac{\alpha_{ar}}{2}} d_{rc}^{\frac{\alpha_{rc}}{2}}}\right) \times \left(\sqrt{P_c} s_c(n) + \sqrt{P_b} s_b(n)\right) + z_c(n), \tag{2}$$

where $P_c = (1-\rho)P_a$ and $P_b = \rho P_a$ are the average transmitted power levels for $s_c(n)$ and $s_b(n)$ $(n = 1, 2, \ldots, N)$, respectively. P_a represents the total transmission power of Alice and ρ indicates power allocation factor, i.e., $0 < \rho < 0.5$. This setup can utilize $s_c(n)$ as a cover for $s_b(n)$. $z_c(n) \sim \mathcal{CN}\left(0, \sigma_c^2\right)$ and $z_b(n) \sim \mathcal{CN}\left(0, \sigma_b^2\right)$ denote the additive white Gaussian noises (AWGNs) for Carol and Bob, respectively. $\Theta_R = \text{diag}\left(\sqrt{\beta_1^r} e^{j\theta_1^r}, \ldots, \sqrt{\beta_k^r} e^{j\theta_k^r}, \ldots, \sqrt{\beta_{K_n}^r} e^{j\theta_{K_n}^r}\right)$ and $\Theta_T = \text{diag}\left(\sqrt{\beta_1^t} e^{j\theta_1^t}, \ldots, \sqrt{\beta_k^t} e^{j\theta_k^t}, \ldots, \sqrt{\beta_{K_m}^t} e^{j\theta_{K_m}^t}\right)$ denote as the reflection and transmission coefficient matrices of STAR-RIS, respectively, where $\sqrt{\beta_k^r}$, $\sqrt{\beta_k^t} \in (0, 1]$, θ_k^r, $\theta_k^t \in [0, 2\pi)$ represent the amplitude and phase shift of the k th STAR-RIS element, respectively. α_i and α_f are the path loss exponents.

C. Detection Metrics at Willie

To detect the existence of covert information, Willie attempts to differentiate the following two hypotheses:

$$y_w(n) = \begin{cases} \left(\frac{h_{aw}}{d_{aw}^{\frac{\alpha_{aw}}{2}}} + \frac{\mathbf{h}_{ar_1}^H \Theta_R \mathbf{h}_{rw}}{d_{ar}^{\frac{\alpha_{ar}}{2}} d_{rw}^{\frac{\alpha_{rw}}{2}}}\right) \times \sqrt{P_c} s_c(n) + z_w(n), & H_0, \\ \left(\frac{h_{aw}}{d_{aw}^{\frac{\alpha_{aw}}{2}}} + \frac{\mathbf{h}_{ar_1}^H \Theta_R \mathbf{h}_{rw}}{d_{ar}^{\frac{\alpha_{ar}}{2}} d_{rw}^{\frac{\alpha_{rw}}{2}}}\right) \times \left(\sqrt{P_c} s_c(n) + \sqrt{P_b} s_b(n)\right) + z_w(n), & H_1, \end{cases} \tag{3}$$

where $z_w(n) \sim \mathcal{CN}\left(0, \sigma_w^2\right)$ is the AWGN at Willie. H_0 and H_1 represent only common signal transmission and joint

common and covert signal transmission, respectively. For convenience, we assume that $\alpha_{ar} = \alpha_{rb} = \alpha_{rc} = \alpha_{aw} = \alpha_{rw} = \alpha_{ab}/2 = \alpha$, $d_{ar}d_{rb} = d_{ab}^2$ and $d_{ar}d_{rc} = d_{ac}^2$.

Using the definition $T_w = \sum_{n=1}^{N} |y_w(n)|^2 \Big/ N$, and letting $N \to \infty$, we can express Willie's average received power as

$$T_w = \begin{cases} \left(\dfrac{|h_{aw}|^2}{d_{aw}^{\alpha}} + \dfrac{\left|\mathbf{h}_{ar_1}^H \Theta_R \mathbf{h}_{rw}\right|^2}{d_{ar}^{\alpha} d_{rw}^{\alpha}} \right) P_c + \sigma_w^2, & H_0, \\ \left(\dfrac{|h_{aw}|^2}{d_{aw}^{\alpha}} + \dfrac{\left|\mathbf{h}_{ar_1}^H \Theta_R \mathbf{h}_{rw}\right|^2}{d_{ar}^{\alpha} d_{rw}^{\alpha}} \right) (P_c + P_b) + \sigma_w^2, & H_1. \end{cases} \tag{4}$$

In the STAR-RIS NOMA network, the decision rule for solving Willie's DEP can be defined by

$$T_w \underset{D_0}{\overset{D_1}{\gtrless}} \eta, \tag{5}$$

where η is the judgment threshold to be determined. D_0 and D_1 indicate decisions in favor of H_0 and H_1, respectively.

III. Performance Analysis and Optimization Strategy

A. Detection Performance at Willie

The prior probabilities of H_0 and H_1 are assumed to be equal. Based on this assumption, Willie's DEP is defined as

$$\xi = \mathbb{P}_f + \mathbb{P}_m, \tag{6}$$

where $\mathbb{P}_f = \Pr(D_1 | H_0)$ and $\mathbb{P}_m = \Pr(D_0 | H_1)$ denote the false alarm probability (FAP) and the missed detection probability (MDP), respectively.

Remark 1. *With the CSI of the Alice-Bob and Alice-STAR-RIS-Bob links, an optimal Θ_R can be designed, such that $\left|\mathbf{h}_{ar_1}^H \Theta_R \mathbf{h}_{rw}\right|^2$ becomes a random variable at Willie, with only the statistical characteristic of $\left|\mathbf{h}_{ar_1}^H \Theta_R \mathbf{h}_{rw}\right|^2$ known to Willie. This ensures a low possibility of discovering the covert communication to Bob. This is because when Willie detects its received power, it cannot determine whether the change in received power is the result of a common signal transmission or a covert signal transmission.*

For convenience, we set $H_K = \mathbf{h}_{ar_1}^H \Theta_R \mathbf{h}_{rw}$. Since Willie has no knowledge of the instantaneous CSI of Alice-STAR-RIS. Therefore, in order to compute the detection performance, according to the central limit theorem (CLT), the cumulative distribution function (CDF) of H_K can be approximated as a complex Gaussian random variable with mean 0 and variance $\lambda_{ar_1}\lambda_{rw}K_n$, i.e., $H_K \sim \mathcal{CN}(0, \lambda_{ar_1}\lambda_{rw}K_n)$ [16]. Next, we have the following characterizations.

Lemma 1. *The DEP at Willie is expressed as*

$$\xi = \begin{cases} 1, & \eta \le Q_1 |h_{aw}|^2 + \sigma_w^2, \\ g_1, & Q_1 |h_{aw}|^2 + \sigma_w^2 < \eta \le Q_2 |h_{aw}|^2 + \sigma_w^2, \\ g_2, & \eta > Q_2 |h_{aw}|^2 + \sigma_w^2, \end{cases} \tag{7}$$

where $g_1 = e^{-\frac{\eta - \sigma_w^2 - Q_1 |h_{aw}|^2}{Q_3}}$, $g_2 = 1 + g_1 - e^{-\frac{\eta - \sigma_w^2 - Q_2 |h_{aw}|^2}{Q_4}}$, $Q_1 = P_c d_{aw}^{-\alpha}$, $Q_2 = (P_c + P_b) d_{aw}^{-\alpha}$, $Q_3 = P_c d_{ar}^{-\alpha} d_{rw}^{-\alpha} \lambda_{ar_1}\lambda_{rw}K_n$, $Q_4 = (P_c + P_b) d_{ar}^{-\alpha} d_{rw}^{-\alpha} \lambda_{ar_1}\lambda_{rw}K_n$.

Proof: The $\mathbb{P}_f = \Pr(T_w > \eta | H_0)$ and the $\mathbb{P}_m = \Pr(T_w < \eta | H_1)$ as well as (6) can be determined readily (under the Gaussian approximation for H_K) to obtain (7). ■

Theorem 1. *Considering the detection metrics above, the optimal judgment threshold for minimizing ξ is given by*

$$\eta^* = \begin{cases} \eta_0, & |h_{aw}|^2 < \dfrac{\eta_0 - \sigma_w^2}{Q_2}, \\ \sigma_w^2 + Q_2 |h_{aw}|^2, & \text{otherwise}, \end{cases} \tag{8}$$

and the corresponding minimum detection error probability (MDEP) can be expressed as

$$\xi^* = \begin{cases} 1 - g_3 + g_4, & |h_{aw}|^2 < \dfrac{\eta_0 - \sigma_w^2}{Q_2}, \\ e^{-\frac{P_b Q_2 |h_{aw}|^2}{(P_b + P_c) Q_3}}, & \text{otherwise}, \end{cases} \tag{9}$$

where $g_3 = e^{-\frac{\eta_0 - \sigma_w^2 - Q_2 |h_{aw}|^2}{Q_4}}$, $g_4 = e^{-\frac{\eta_0 - \sigma_w^2 - Q_1 |h_{aw}|^2}{Q_3}}$, $\eta_0 = \sigma_w^2 + [Q_3 Q_4 \ln(Q_3/Q_4)] / (Q_3 - Q_4)$.

Proof: See Appendix A. ■

Alice does not have known the instantaneous CSI regarding of h_{aw} and we use the average minimum detection error probability (AMDEP) with respect to $|h_{aw}|^2$ as a performance evaluation metric. Under the optimal judgment threshold, the AMDEP can be easily obtained utilizing the total probability theorem.

Theorem 2. *Willie's AMDEP is obtained as (10), which is shown at the top of the next page.*

B. Outage Probability Analysis

According to the NOMA protocol, Bob first decodes Carol's signal, then removes it from the received signal and detects its own signal. Thus, the signal-to-interference-plus-noise ratio (SINR) for decoding $s_c(n)$ and $s_b(n)$ at Bob can be expressed as

$$\gamma_{b \to c} = \frac{(1 - \rho)\mu_1 \left| h_{ab} + \mathbf{h}_{ar_1}^H \Theta_R \mathbf{h}_{rb} \right|^2 d_{ab}^{-2\alpha}}{\rho \mu_1 \left| h_{ab} + \mathbf{h}_{ar_1}^H \Theta_R \mathbf{h}_{rb} \right|^2 d_{ab}^{-2\alpha} + 1}, \tag{11}$$

and

$$\gamma_b = \frac{\rho \mu_1 \left| h_{ab} + \mathbf{h}_{ar_1}^H \Theta_R \mathbf{h}_{rb} \right|^2 d_{ab}^{-2\alpha}}{\varpi (1 - \rho)\mu_1 \left| h_{ab} + \mathbf{h}_{ar_1}^H \Theta_R \mathbf{h}_{rb} \right|^2 d_{ab}^{-2\alpha} + 1}, \tag{12}$$

where $\mu_1 = P_a/\sigma_b^2$ denotes the average transmitted signal-to-noise ratio (SNR) from Alice to Bob. $\varpi \in [0, 1]$ stands for the coefficient of imperfect SIC due to implementation issues such as shadow decline and error propagation [17].

Similarly, the SINR for decoding Carol's own information is given by

$$\gamma_c = \frac{(1 - \rho)\mu_2 \left| h_{ac} + \mathbf{h}_{ar_2}^H \Theta_T \mathbf{h}_{rc} \right|^2 d_{ac}^{-2\alpha}}{\rho \mu_2 \left| h_{ac} + \mathbf{h}_{ar_2}^H \Theta_T \mathbf{h}_{rc} \right|^2 d_{ac}^{-2\alpha} + 1}, \tag{13}$$

where $\mu_2 = P_a/\sigma_c^2$ is expressed as the average transmitted SNR from Alice to Carol.

$$\bar{\xi}^{*}=\left\{1+\frac{Q_3}{Q_1\lambda_{aw}-Q_3}\left[e^{\frac{(Q_2\lambda_{aw}-Q_1\lambda_{aw}+Q_3)\left(\sigma_w^2-\eta_0\right)}{Q_2Q_3\lambda_{aw}}}-e^{\frac{\sigma_w^2-\eta_0}{Q_3}}\right]-\frac{Q_4}{Q_2\lambda_{aw}-Q_4}\left(e^{\frac{\sigma_w^2-\eta_0}{Q_2\lambda_{aw}}}-e^{\frac{\sigma_w^2-\eta_0}{Q_4}}\right)\right\}\left(1-e^{\frac{\sigma_w^2-\eta_0}{Q_2\lambda_{aw}}}\right)$$
$$+\frac{\left(P_c+P_b\right)Q_3}{P_bQ_2\lambda_{aw}+\left(P_c+P_b\right)Q_3}e^{\frac{\left(\sigma_w^2-\eta_0\right)\left[P_bQ_2\lambda_{aw}+2\left(P_c+P_b\right)Q_3\right]}{\left(P_c+P_b\right)Q_2Q_3\lambda_{aw}}} \tag{10}$$

According to [16], $\left|h_{ab}+\mathbf{h}_{ar_1}^H\Theta_R\mathbf{h}_{rb}\right|^2$ obeys an exponential distribution with a parameter of $\lambda=\lambda_{ab}+\lambda_{ar_1}\lambda_{rb}K_n$, then we can obtain the CDF of $\left|h_{ab}+\mathbf{h}_{ar_1}^H\Theta_R\mathbf{h}_{rb}\right|^2$. We following derive the OP to measure the system reliability.

Lemma 2. *The OPs of Bob and Carol are respectively expressed as*

$$\delta_b=\begin{cases}1, & \rho\geq\phi_1 \text{ or } \rho\leq\phi_2,\\ 1-e^{-\frac{\gamma_c^{th}}{\left(\lambda_{ab}+\lambda_{ar_1}\lambda_{rb}K_n\right)\Delta_1\mu_1d_{ab}^{-2\alpha}}}, & \Delta_3<\rho<\phi_1,\\ 1-e^{-\frac{\gamma_b^{th}}{\left(\lambda_{ab}+\lambda_{ar_1}\lambda_{rb}K_n\right)\Delta_2\mu_1d_{ab}^{-2\alpha}}}, & \phi_2<\rho\leq\Delta_3,\end{cases} \tag{14}$$

and

$$\delta_c=\begin{cases}1, & \rho\geq\phi_1 \text{ or } \rho=0,\\ 1-e^{-\frac{\gamma_c^{th}}{\left(\lambda_{ac}+\lambda_{ar_2}\lambda_{rc}K_m\right)\Delta_1\mu_2d_{ac}^{-2\alpha}}}, & 0<\rho<\phi_1,\end{cases} \tag{15}$$

where $\gamma_b^{th}=2^{R_b}-1$, $\gamma_c^{th}=2^{R_c}-1$, *while* R_b *and* R_c *are the predefined target rates for signals* s_b *and* s_c *respectively.* $\phi_1=1/\left(1+\gamma_c^{th}\right)$, $\phi_2=\varpi\gamma_b^{th}/\left(1+\varpi\gamma_b^{th}\right)$, $\Delta_1=1-\rho-\rho\gamma_c^{th}$, $\Delta_2=\rho-\varpi\left(1-\rho\right)\gamma_b^{th}$ *and* $\Delta_3=\left(\gamma_b^{th}+\varpi\gamma_b^{th}\gamma_c^{th}\right)/\left(\gamma_c^{th}+\gamma_b^{th}+\gamma_c^{th}\gamma_b^{th}+\varpi\gamma_b^{th}\gamma_c^{th}\right)$.

Proof: An outage event occurs at Bob when it can not recover $s_b\left(n\right)$ at Bob or when Bob fails to decode $s_c\left(n\right)$. Hence, the OP at Bob can be expressed as

$$\begin{aligned}\delta_b&=\Pr\left(\gamma_{b\to c}<\gamma_c^{th}\right)+\Pr\left(\gamma_b<\gamma_b^{th},\gamma_{b\to c}>\gamma_c^{th}\right)\\&=1-\Pr\left(\gamma_{b\to c}>\gamma_c^{th},\gamma_b>\gamma_b^{th}\right)\\&=1-\Pr\left(\Delta_1\left|h_{ab}+\mathbf{h}_{ar_1}^H\Theta_R\mathbf{h}_{r_1w}\right|^2>\frac{\gamma_c^{th}}{\mu_1d_{ab}^{-2\alpha}},\right.\\&\qquad\left.\left|h_{ab}+\mathbf{h}_{ar_1}^H\Theta_R\mathbf{h}_{r_1w}\right|^2>\frac{\gamma_b^{th}}{\mu_1\Delta_2d_{ab}^{-2\alpha}}\right)\end{aligned} \tag{16}$$

Case 1: When $\rho\geq\phi_1$ or $\rho\leq\phi_2$, we have $\delta_b=1$.

Case 2: When $\Delta_3<\rho<\phi_1$, the OP can be derived as

$$\begin{aligned}\delta_b=&1-\Pr\left(\left|h_{ab}+\mathbf{h}_{ar_1}^H\Theta_R\mathbf{h}_{rw}\right|^2>\frac{\gamma_c^{th}}{\mu_1\Delta_1d_{ab}^{-2\alpha}}\right)\\=&1-\int_{\frac{\gamma_c^{th}}{\mu_1\Delta_1d_{ab}^{-2\alpha}}}^{\infty}f_{\left|h_{ab}+\mathbf{h}_{ar_1}^H\Theta_R\mathbf{h}_{rw}\right|^2}\left(x\right)\mathrm{d}x\end{aligned} \tag{17}$$

Case 3: When $\phi_2<\rho\leq\Delta_3$, we have $\delta_b=1-\Pr\left(\left|h_{ab}+\mathbf{h}_{ar_1}^H\Theta_R\mathbf{h}_{rw}\right|^2>\gamma_b^{th}/\left(\mu_1\Delta_2d_{ab}^{-2\alpha}\right)\right)$. The proof is similar to *Case 2*.

The outage event occurs when Carol fails to decode $s_c\left(n\right)$, which can be represented by $\delta_c=\Pr\left(\gamma_c<\gamma_c^{th}\right)$. **Lemma 2** can be obtained through the above series of calculations. ■

C. Maximization of the Effective Covert Rate

In this subsection, we optimize the covertness performance of Bob while ensuring the reliability requirement of Carol and the covertness requirement of the STAR-RIS NOMA networks. We introduce the ECR, defined as $\Upsilon=R_b\left(1-\delta_b\right)$, as a metric of the covertness performance of Bob. Then, the optimization problem that maximizes the ECR is given by

$$\begin{aligned}&\max_{\rho}\ \Upsilon=R_b\left(1-\delta_b\right)\\&\text{s.t}\quad\bar{\xi}^{*}\geq1-\varepsilon\\&\qquad\delta_c\leq\delta_{th}\end{aligned} \tag{18}$$

where ε is a pre-determined covertness threshold and its value is sufficiently small, and δ_{th} denotes the maximum allowed OP at Carol.

Theorem 3. *For a given covertness constraint* ε *and a reliability constraint* δ_{th}*, the optimal power allocation factor* ρ *for maximizing the ECR is given as*

$$\rho^{*}=\min\left(\rho_\delta,\rho_\varepsilon,\Delta_3\right). \tag{19}$$

where ρ_ε *is the solution of* $\bar{\xi}^{*}=1-\varepsilon$ *for* ρ*, and* ρ_δ *is the solution to* $\delta_c=\delta_{th}$ *for* ρ*.*

Proof: For a given ε, $\bar{\xi}^{*}$ is a decreasing function of ρ in Eq. (10). We can obtain the maximum ρ, i.e. ρ_ε (ρ_ε is the solution of $\bar{\xi}^{*}=1-\varepsilon$). Similarly, for a given δ_{th}, δ_c is a increasing function of ρ in Eq. (15). We can obtain the maximum ρ, i.e. ρ_δ (ρ_δ is the solution to $\delta_c=\delta_{th}$). Therefore, $\rho\leq\min\left(\rho_\varepsilon,\rho_\delta\right)$ can be obtained by concurrently satisfying the above two constraints. Furthermore, since there are different intervals for δ_b, the optimal factor $\rho^{*}=\min\left(\rho_\delta,\rho_\varepsilon,\Delta_3\right)$ can be obtained by analysing the following two cases i) $\Delta_3\leq\min\left(\rho_\delta,\rho_\varepsilon\right)<\phi_1$ and ii) $\phi_2<\min\left(\rho_\delta,\rho_\varepsilon\right)\leq\Delta_3$, which concludes the proof. ■

IV. Numerical Analysis

In this section, numerical results are provided to verify the detection performance of Willie and the covertness performance of the system under consideration. The simulation parameters are set to $\lambda_{ar_{1/2}}=1.6$, $\lambda_{ab}=2$, $\lambda_{ac}=2.6$, $\lambda_{rb}=\lambda_{rw}=2.2$, $\lambda_{rc}=\lambda_{aw}=3$. $d_{ar}=5$ m, $d_{aw}=d_{rc}=3$ m, $d_{rb}=d_{rw}=4$ m. $\alpha=2.5$, $R_c=R_b=1$ bps/Hz, $\sigma_b^2=\sigma_c^2=\sigma_w^2=-20$ dB [18].

Fig. 2 depicts the DEP as a function of the judgment threshold η for different transmission power P_a. We set $K_n=64$ and $\rho=0.4$. Firstly, the result shows that the DEP first decreases and then increases as η increases. Hence, there exists a minimum DEP. Furthermore, it is observed that the simulation curves are in perfect agreement with the theoretical

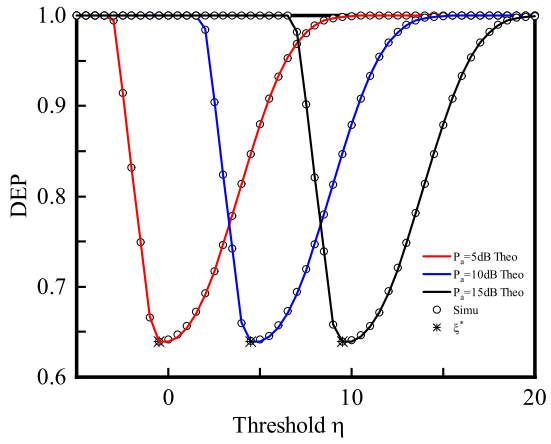

Fig. 2. DEP versus η for the comparison of different P_a.

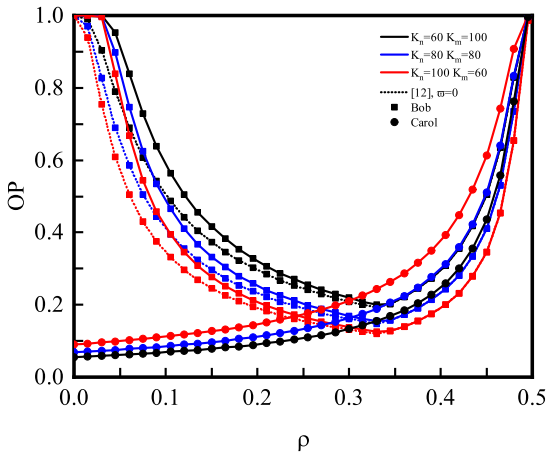

Fig. 4. OP versus ρ for different values of K_n and K_m.

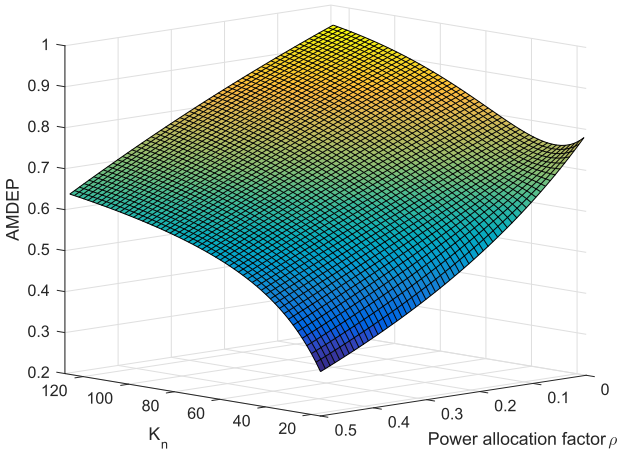

Fig. 3. AMDEP versus K_n and ρ.

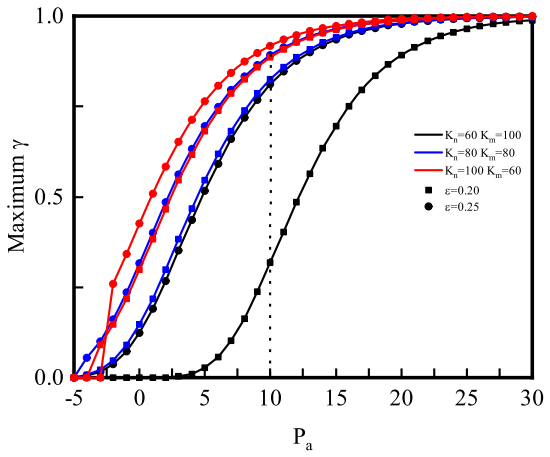

Fig. 5. Maximum Υ versus P_a for different values of ε, K_n and K_m.

ones, thus verifying the characterization in **Lemma 1**. We also find that although the optimal judgment thresholds to achieve the minimum of ξ (i.e., ξ^*) are different, ξ^* has the same value in different transmission power options, verifying the result in **Theorem 1**. In addition, it can be further observed that the DEP varies significantly with the judgment threshold, which illustrates the importance of optimizing the judgment threshold at Willie.

In Fig. 3, we demonstrate the three-dimensional relationship between AMDEP and different ρ and the number of elements K_n, used by STAR-RIS for reflection. We first observe that AMDEP decreases as ρ increases. This is because the larger ρ is, the more transmission power is allocated to Bob, causing P_b to increase, making it more likely for Willie to detect the covert communication process. It is worth noting that P_a has no effect on AMDEP. According to the NOMA principle, it can be readily seen from (10) that AMDEP is only a function of ρ and K_n. Furthermore, for a fixed ρ, AMDEP increases with increasing K_n. This can be attributed to the fact that the increase in ρ helps to generate a large STAR-RIS phase shift uncertainty to confuse Willie and thus worsen detection performance of Willie.

Fig. 4 shows the curves of OP versus ρ for different users. We set $\varpi = 0.02$. It can be observed that Bob's OP first decreases and then fast increases with the increase of ρ. When $\rho = \Delta_3$, the OP of Bob reaches the minimum value. This is because according to the NOMA principle, Bob needs to decode the public signal $s_c(n)$ before decoding its own signal $s_b(n)$. When $\rho \to 0$, the transmitted power of $s_c(n)$ is the maximum and Carol has the best communication quality. In this case, the transmitted power of $s_b(n)$ is minimum, resulting in $\delta_b \to 1$. With the increase of ρ, the transmitted power of $s_c(n)$ will decrease, and $\delta_c \to 1$ when $\rho \to 1/(1+\gamma_c^{th})$. Within this range, there must be some value that makes the OP of Bob minimum. Furthermore, perfect SIC can better improve the system performance. When when Bob has perfect SIC, its OP is lower than that of imperfect SIC.

Fig. 5 plots the variation of the maximum Υ versus different transmission power P_a under ε and the number of elements K_n and K_m of STAR-RIS serving Bob and Carol, respectively. We set $K = 160\,(K = K_n + K_m)$, $\varpi = 0.01$ and $\delta_{th} = 0.3$. We can observe that the maximum Υ is positively

correlated with P_a and ε. As P_a increases, maximal Υ tends to a constant value. In addition, increasing K_n significantly increases the maximum Υ when ε and P_a are fixed constants. This is because the higher the number of elements used for reflection in STAR-RIS, and the higher the number of covert signals received by Bob, which ultimately leads to an increase in the maximum Υ. When P_a is fixed, the optimal power allocation factor corresponding to the maximum Υ can be obtained, which verifies the analysis of **Theorem 3**, i.e. $\rho^* = \min(\rho_\delta, \rho_\varepsilon, \Delta_3)$. Furthermore, higher levels of cover performance can be achieved by setting different numbers of reflection and transmission elements in the STAR-RIS NOMA networks.

V. Conclusion

This paper investigated the covertness performance of STAR-RIS NOMA networks by deriving analytical expressions for the DEP, AMDEP and OP. To be pratical, the assumption of imperfect SIC is taken into consideration. An ECR maximization problem was then developed to balance the reliability and covertness of the considered network. Finally, in the numerical results, the influence of Alice's transmit power, power allocation factor, covertness constraint and STAR-RIS element number on the covertness performance of the proposed system was investigated. Moreover, the maximum ECR converges to a specific constant when Alice's transmit power is sufficiently large. Our work provided a beneficial theoretical reference for the study of covert communication systems. It can also be extended to enable multi-user covert communication in the STAR-RIS NOMA networks, which will be focused in our future research works.

APPENDIX A

Based on (7), we seek to find the optimal judgment threshold that minimizes DEP.

Case 1: When $\eta \leq Q_1|h_{aw}|^2 + \sigma_w^2$, $\xi = 1$, there is no optimal η.

Case 2: When $Q_1|h_{aw}|^2 + \sigma_w^2 < \eta \leq Q_2|h_{aw}|^2 + \sigma_w^2$, ξ is a monotonically decreasing function with respect to η, so $\eta^* = Q_2|h_{aw}|^2 + \sigma_w^2$ is chosen as the optimal judgment threshold that minimizes ξ.

Case 3: When $\eta > Q_2|h_{aw}|^2 + \sigma_w^2$, we derive the first order derivative of ξ with respect to η, which is expressed as

$$\frac{\partial \xi}{\partial \eta} = \frac{1}{Q_4} e^{\frac{\sigma_w^2 + Q_2|h_{aw}|^2 - \eta}{Q_4}} - \frac{1}{Q_3} e^{\frac{\sigma_w^2 + Q_1|h_{aw}|^2 - \eta}{Q_3}}. \quad (20)$$

Letting (20) be equal to 0, we can get to the solution as $\eta_0 = \sigma_w^2 + [Q_3 Q_4 \ln(Q_3/Q_4)] / (Q_3 - Q_4)$. By using the results of (20) and η_0, we explore the monotonicity of ξ as follows:

1) When $\eta_0 > Q_2|h_{aw}|^2 + \sigma_w^2$, for $Q_2|h_{aw}|^2 + \sigma_w^2 < \eta < \eta_0$, $\partial \xi / \partial \tau < 0$, so ξ is decreasing monotonically with η. However, for $\eta_0 \leq \eta < +\infty$, ξ increases as η increases, and hence the optimal judgment threshold to minimize Willie's DEP is η_0.

2) When $\eta_0 \leq Q_2|h_{aw}|^2 + \sigma_w^2$, for $\eta > Q_2|h_{aw}|^2 + \sigma_w^2$, ξ is a monotonically increasing function, and therefore $\eta^* = Q_2|h_{aw}|^2 + \sigma_w^2$ is the optimal judgment threshold to minimize DEP.

The optimal judgment threshold for each case is brought into (7) to obtain the corresponding MDEP. With the above characterizations, the proof of **Theorem 1** is completed.

References

[1] C. Huang, A. Zappone, G. C. Alexandropoulos, M. Debbah, and C. Yuen, "Reconfigurable intelligent surfaces for energy efficiency in wireless communication," *IEEE Trans. Wireless Commun.*, vol. 18, no. 8, pp. 4157–4170, Aug. 2019.

[2] Y. Liu, X. Mu, J. Xu, R. Schober, Y. Hao, H. V. Poor, and L. Hanzo, "STAR: Simultaneous transmission and reflection for 360°coverage by intelligent surfaces," *IEEE Wireless Commun.*, vol. 28, no. 6, pp. 102–109, Dec. 2021.

[3] J. Zuo, Y. Liu, Z. Ding, and L. Song, "Simultaneously transmitting and reflecting (STAR) RIS assisted NOMA systems," in *Proc. IEEE Glob. Commun. Conf.*, Madrid, Spain, 2021, pp. 1–6.

[4] Y. Yuan, S. Wang, Y. Wu, H. V. Poor, Z. Ding, X. You, and L. Hanzo, "NOMA for next-generation massive IoT: Performance potential and technology directions," *IEEE Commun. Mag.*, vol. 59, no. 7, pp. 115–121, Jul. 2021.

[5] X. Li, X. Gao, L. Yang, H. Liu, J. Wang, and K. M. Rabie., "Performance analysis of STAR-RIS-CR-NOMA based consumer IoT networks for resilient industry 5.0," *IEEE Trans. Consum. Electron.*, pp. 1–1, Sep. 2023.

[6] C. Zhang, W. Yi, Y. Liu, Z. Ding, and L. Song, "STAR-IOS aided NOMA networks: channel model approximation and performance analysis," *IEEE Trans. Wireless Commun.*, vol. 21, no. 9, pp. 6861–6876, Sep. 2022.

[7] X. Yue, J. Xie, Y. Liu, Z. Han, R. Liu, and Z. Ding, "Simultaneously transmitting and reflecting reconfigurable intelligent surface assisted NOMA networks," *IEEE Trans. Wireless Commun.*, vol. 22, no. 1, pp. 189–204, Jan. 2023.

[8] H. Liu, G. Li, X. Li, Y. Liu, G. Huang, and Z. Ding, "Effective capacity analysis of STAR-RIS assisted NOMA networks," *IEEE Wireless Commun. Lett.*, vol. 11, no. 9, pp. 1930–1934, Sept. 2022.

[9] T. Wang, M.-A. Badiu, G. Chen, and J. P. Coon, "Outage probability analysis of STAR-RIS assisted NOMA network with correlated channels," *IEEE Commun. Lett.*, vol. 26, no. 8, pp. 1774–1778, Aug. 2022.

[10] X. Li, Y. Zheng, M. Zeng, Y. Liu, and O. A. Dobre, "Enhancing secrecy performance for STAR-RIS NOMA networks," *IEEE Trans. Veh. Technol.*, vol. 72, no. 2, pp. 2684–2688, Feb. 2023.

[11] L. Tao, W. Yang, S. Yan, D. Wu, X. Guan, and D. Chen, "Covert Communication in Downlink NOMA Systems With Random Transmit Power," *IEEE Wireless Commun. Lett.*, vol. 9, no. 11, pp. 2000–2004, Nov. 2020.

[12] Y. Zhang, W. He, X. Li, H. Peng, K. Rabie, G. Nauryzbayev, B. M. ElHalawany, and M. Zhu, "Covert communication in downlink NOMA systems with channel uncertainty," *IEEE Sens. J.*, vol. 22, no. 19, pp. 101–112, Oct. 2022,.

[13] X. Lu, E. Hossain, T. Shafique, S. Feng, H. Jiang, and D. Niyato, "Intelligent reflecting surface enabled covert communications in wireless networks," *IEEE Network*, vol. 34, no. 5, pp. 148–155, Sept. 2020.

[14] L. Lv, Q. Wu, Z. Li, Z. Ding, N. Al-Dhahir, and J. Chen, "Covert communication in intelligent reflecting surface-assisted NOMA systems: Design, analysis, and optimization," *IEEE Trans. Wireless Commun.*, vol. 21, no. 3, pp. 1735–1750, Mar. 2022.

[15] S. Fang, G. Chen, Z. Abdullah, and Y. Li, "Intelligent omni surface-assisted secure mimo communication networks with artificial noise," *IEEE Commun. Lett.*, vol. 26, no. 6, pp. 1231–1235, Jun. 2022.

[16] Z. Ding, R. Schober, and H. V. Poor, "On the impact of phase shifting designs on irs-noma," *IEEE Wireless Commun. Lett.*, vol. 9, no. 10, pp. 1596–1600, Oct. 2020.

[17] N. S. Mouni, A. Kumar, and P. K. Upadhyay, "Adaptive user pairing for NOMA systems with imperfect SIC," *IEEE Wireless Commun. Lett.*, vol. 10, no. 7, pp. 1547–1551, Jul. 2021.

[18] S. Ma, Y. Zhang, H. Li, J. Sun, J. Shi, H. Zhang, C. Shen, and S. Li, "Covert beamforming design for intelligent-reflecting-surface-assisted IoT networks," *IEEE Internet Things J.*, vol. 9, no. 7, pp. 5489–5501, Apr. 2022.